

DESIGN OF PENETRATIONS IN HADRON SHIELDS

P. J. Gollon and M. Awschalom

National Accelerator Laboratory *)
Batavia, Illinois 60510, U.S.A.

1. INTRODUCTION

Among the various problems involved in the design of accelerator radiation shielding, the problem of personnel and vehicle penetrations has received the least attention in the shielding literature. The removal of mass from a hadron shield to construct an access to its interior weakens the shield in two ways:

- i) it removes absorber from the shield, reducing the effectiveness of the shield in the regions of the penetration (see Fig. 1),
- ii) it provides a leakage path for neutrons.

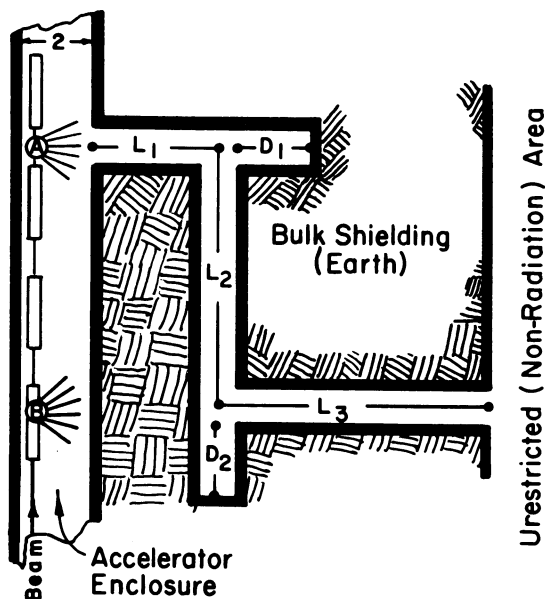


Fig. 1 Typical multi-leg penetration used in neutron dose attenuation calculations.

*) Operated by Universities Research Association, Inc., under contract with the U.S. Atomic Energy Commission.

The obvious solution, that of making the penetration "long" and "full of bends", is costly and inconvenient. One would prefer to minimize both the length and cost of the penetration without compromising radiation safety.

Calculating the neutron dose rate outside a penetration may be divided rather cleanly into two parts:

- i) establishing a reasonable neutron source location, intensity and energy spectrum so that one may calculate the neutron dose entering the penetration,
- ii) calculating the neutron flux and/or dose attenuation in the penetration itself.

In what follows we will assume that the shield is not significantly weakened by the removal of mass from the region of the penetration, and will be concerned only with the leakage of neutrons through the penetration.

2. NEUTRON SOURCE TERM

Interacting high-energy protons initiate extranuclear cascades. The neutron component of the hadron cascade is the most significant in terms of its ability to penetrate both the bulk shielding and the penetrations in that shielding. Predictable beam losses will occur at extraction septa, beam scrapers, beam dumps, etc. Such loss points will be surrounded by local shielding, so that no additional bulk shielding will be required. Therefore, they present no special shielding problems.

It is far more difficult to attempt to predict the location and intensity of so-called "unpredictable" beam losses. The model adopted at NAL for such "unpredictable" beam losses is:^{1,2)}

- i) Losses occur at discrete points, rather than uniformly around the synchrotron.
- ii) Losses occur in every bending magnet, and at the same position in each magnet. (Spacing the loss points regularly facilitates the integration over several

adjacent sources when designing the hadron shield).

iii) The average loss per magnet is the total unpredictable beam loss (calculated by accelerator theorists) divided by the number of magnets. For the two NAL synchrotrons, the relevant parameters are¹⁾

	8-GeV <u>Booster</u>	200-GeV <u>Main Accelerator</u>
Nominal power	19.2	480 kW
General losses (0.1%)	1.92×10^{-2}	0.48 kW
Number of magnets	96	954
Loss per magnet	2×10^{-4}	5×10^{-4} kW

iv) Beam lost in individual magnets varies upwards or downwards (in an unpredictable fashion) from the average by at most a factor of ten³⁾.

v) Self-shielding in the magnets will vary depending on the location of the loss point. The worst case is when self-shielding is negligible. In the most favorable case, the 8" thick back legs of the main accelerator magnets provide an additional attenuation of less than 4. Self-shielding is therefore ignored in these calculations.

vi) The polar angular distribution of the radiation dose around the loss point was taken from the thin target work of Charalambus, et al.⁴⁾.

The more recent and more appropriate thick target dose distribution measurements of Levine, et al⁵⁾ agrees reasonably well with the measurements of Charalambus at small angles from the beam direction, but is a factor of about 3 higher at large angles. This is significant since it has been shown⁶⁾ that the large-angle flux contributes most to the exposure rate outside a cylindrical hadron shield, and we shall see that the same holds true for radiation leaking through a labyrinth⁷⁾.

vii) The overall normalization of the formula relating dose rate to beam loss was based on work done at RHEL and

ANL^{2,8)}.

The source term so derived²⁾ was used as input to the design of the bulk hadron shield and penetrations through it.

2.1 Bulk Hadron Shield

The part of the problem relating to lateral bulk shielding has been treated theoretically by K. O'Brien⁹⁾, R. G. Alsmiller and collaborators¹⁰⁾, J. Ranft¹¹⁾ and A. Van Ginneken¹²⁾. Extensive experimental data is also available from the CERN-LRL-RHEL collaboration³⁾. The above work provides us with the information needed to calculate the dose attenuation of a thick hadron shield to within an order of magnitude for shields with attenuations up to 7 or 8 orders of magnitude.

3. NEUTRON ATTENUATION CALCULATIONS

We were fortunate to obtain for our neutron flux attenuation calculations the program ZEUS ALB.5 written by F. Gervaise and M.-M. d'Hombres^{13,14)}. Their reports presented the results of some calculations and comparison with measurements which indicated the power of the program. The rest of this paper is a discussion of their method and some of the results we have obtained with it. Our main contribution to the program has been to add some diagnostics and correct two mathematical mistakes and some programming errors.

3.1 Theory of the calculation

The power of the Monte Carlo method and ZEUS in particular lies in the generality of the penetration geometries it can treat. ZEUS allows the concrete penetration walls to be an arbitrary assemblage of plane or quadratic surfaces. Mono-energetic neutrons with any one energy from 250-KeV to 8-MeV as chosen by the user are emitted isotropically from a source plane of adjustable dimensions. The neutrons are carried forward until they strike a wall or,

ocasionally, until they are scattered by the air. In the case of a wall scattering, the outgoing direction is chosen randomly according to the Maerker and Muckenthaler parameterization of the neutron dose albedo¹⁵⁾. The usual techniques are used for biasing, splitting and "Russian roulette".

The dose albedo technique used keeps the neutrons monoenergetic in their scatterings. However, we have found the calculated labyrinth attenuation to be insensitive to the energy group used. All calculations described below were done using 3 to 4-MeV neutrons.

3.2 Long straight penetrations

3.2.1 Point source on axis

The simplest calculations involved a section of mock accelerator enclosure (Fig. 2) 2 units wide with a long rectangular penetration perpendicular to it. The enclosure height was adjusted to equal the penetration height. All dimensions are given in units of the square root of the most commonly used cross-sectional area of the penetration. This facilitates the use of a simple scaling rule: if air scattering can be neglected, then scaling a penetration geometry up or down by multiplying all dimensions by a constant does not change the attenuation of that penetration. Note that a) the region of the neutron source must also be scaled, and b) attenuation here means $\phi(\text{in})/\phi(\text{out})$, where these are the doses measured at the entrance and exit of the penetration.

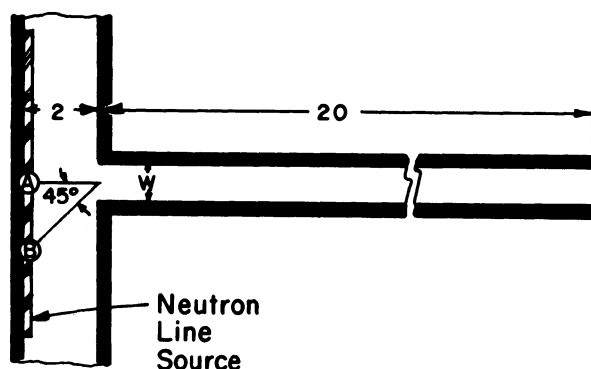


Fig. 2 Long straight labyrinth. Locations of point neutron sources on axis ("A") and off axis ("B") and a line source are shown.

An isotropic "point" source was placed at position "A", looking straight down the penetration. Fig. 3 shows the flux at various distances down square penetrations of height and width of 1 and 2 units. Both curves are similar, and proportional to R^{-2} at large distances from the source. The penetration with the larger width has less attenuation because the scattered component of the flux falls off more slowly.

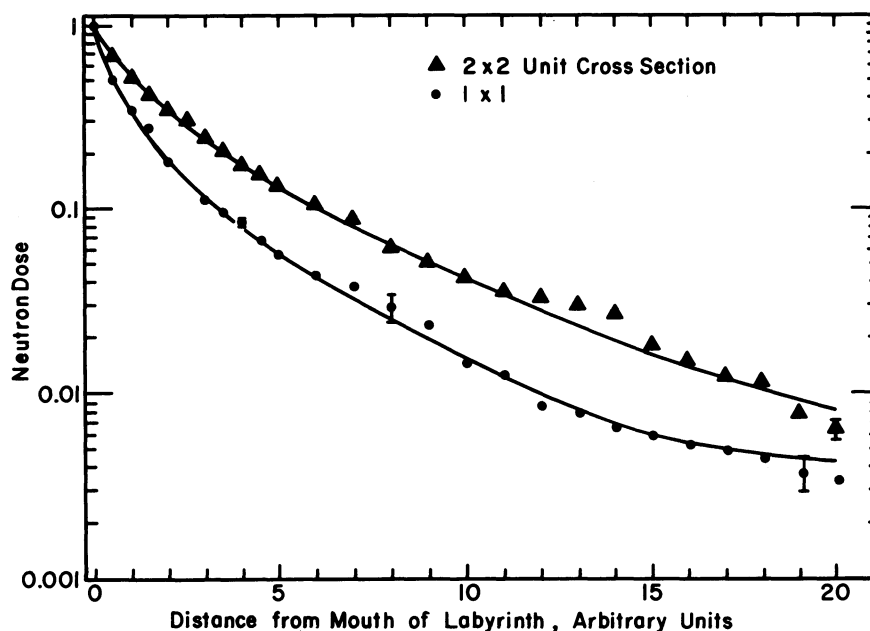


Fig. 3 Calculated neutron dose in straight square penetrations of two different cross-sections.

Also considered were cases in which the cross-sectional area of the penetration was kept constant at one square unit, but the aspect ratio (height/width) changed from 1:1 to 2:1 and 4:1. The results (Fig. 4) are nearly identical. Most of the difference between the sets of points can be attributed to statistical uncertainties in the Monte Carlo calculation. Calculations with multi-leg penetrations also give results nearly independent of aspect ratio.

It is worth noting that the error bars in the figures represent one standard deviation from the calculated mean;

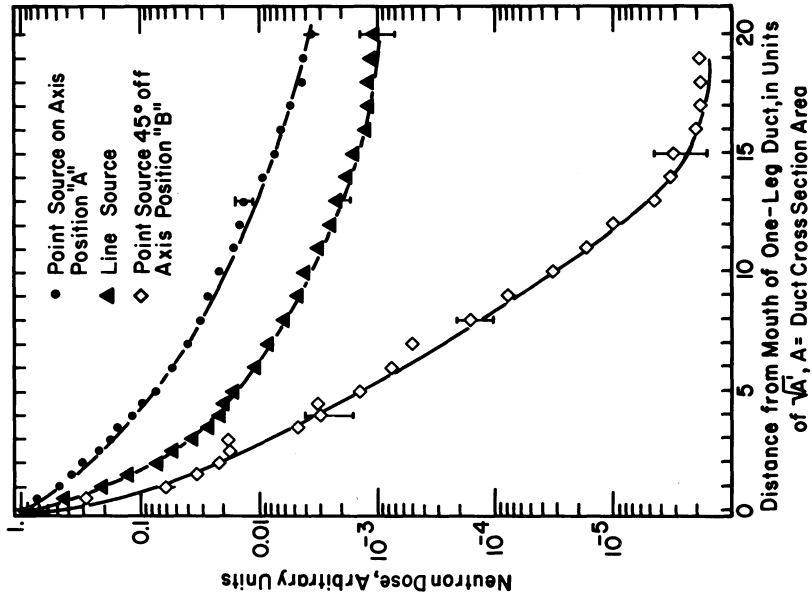


Fig. 5 Neutron dose in a straight penetration with 2:1 aspect ratio for different neutron source locations.

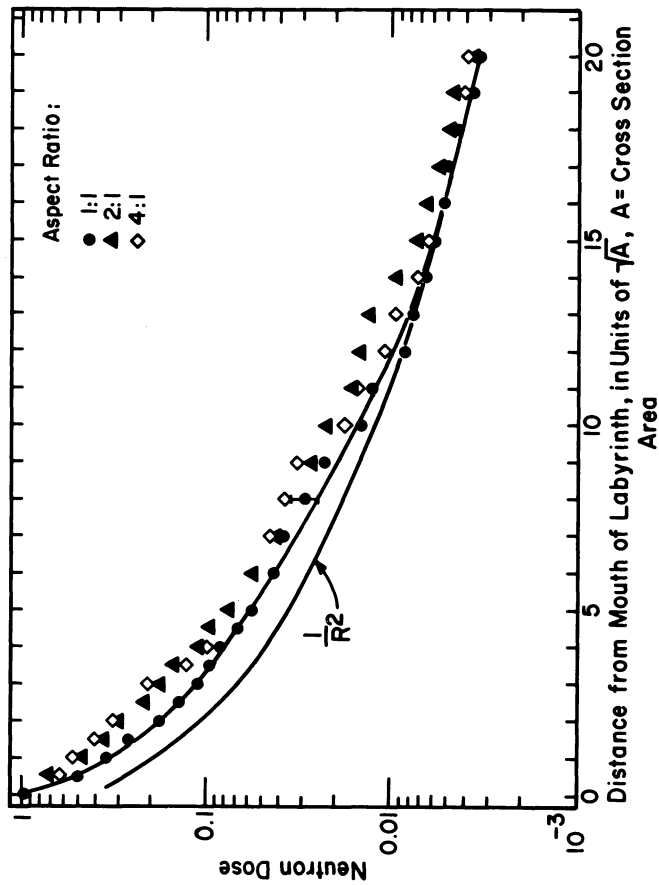


Fig. 4 Neutron dose in straight penetrations of unit area and different aspect ratios (height/width).

this is always less than the standard deviation from the true value. Only in the limit of large number of trials do the calculated mean and standard deviation from it approach the true value and standard deviation from it. This is true for all types of measurements, but it is especially important in Monte Carlo calculations of small quantities.

Also shown in Fig. 4 is an R^{-2} curve matched to the (mostly unscattered) flux at the far end of the tunnel.

3.2.2 Line source and point source off axis

While the point sources on axis provide a "worst case" situation, more realistic situations may involve either a beam loss located away from the penetration axis, or a continuous beam loss (line source). These source locations are illustrated in Fig. 2. Fig. 5 compares the flux attenuation curves obtained from an off-axis point and a line source with the neutron flux from a worst-case, on-axis source.

3.3 Multi-leg labyrinths: conventional geometry

Fig. 1 illustrates a typical three-legged labyrinth, with legs of length L_1 , L_2 , L_3 . Two cul-de-sacs, or "neutron traps" of depth D_1 and D_2 are also shown. We have investigated the effects of leg length, presence and depth of cul-de-sacs, and aspect ratio. The results of some of these calculations are shown in Figs. 6, 7, 8.

Some conclusions and design guidelines are:

- i) The aspect ratio does not significantly affect the attenuation of the penetration.
- ii) A penetration of small cross-section is more "efficient", i.e., has a greater attenuation per foot of length.
- iii) The flux in the first leg falls off as shown in Fig. 4 when the source is on axis.

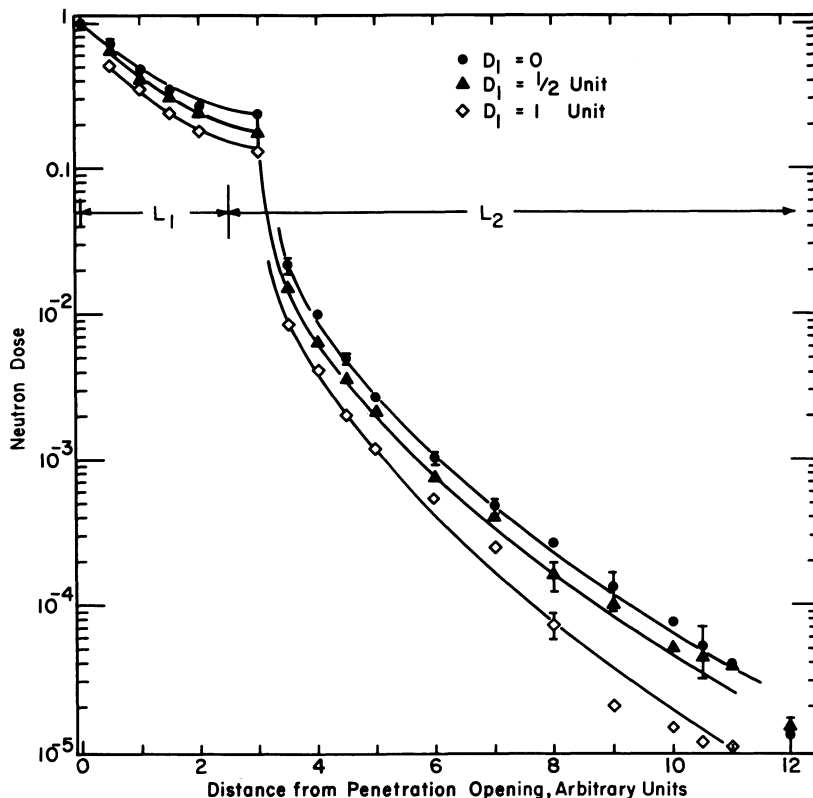


Fig. 6 Neutron dose in a two-legged labyrinth with a cul-de-sac of varying depth at the end of the first leg whose length $L_1 = 2.5\sqrt{A}$.

- iv) As many single-leg flux attenuation curves as needed can be suitably matched together to give the overall attenuation of a multi-leg penetration.
- v) With no cul-de-sacs, the second and every succeeding leg have the same flux attenuation curve.
- vi) A cul-de-sac one unit deep reduces the flux in the following leg by a factor of 2.5 to 3. Shallower ones have a lesser effect.
- vii) An efficient multi-leg penetration will have at least three legs, each bend having a cul-de-sac of depth \sqrt{A} .

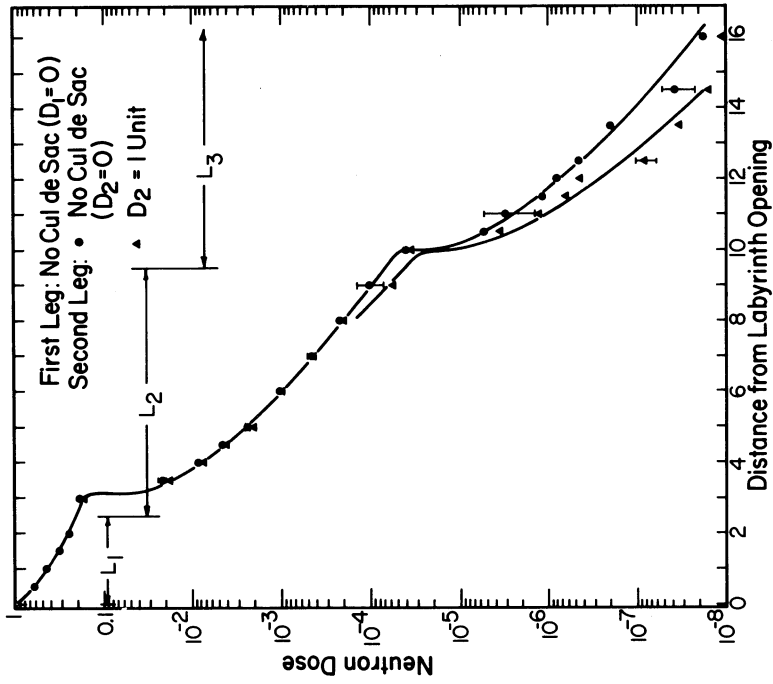


Fig. 8 Neutron dose in a three-legged labyrinth ($L_1 = 2.5$, $L_2 = 14$) with and without a cul-de-sac at the end of the second leg.

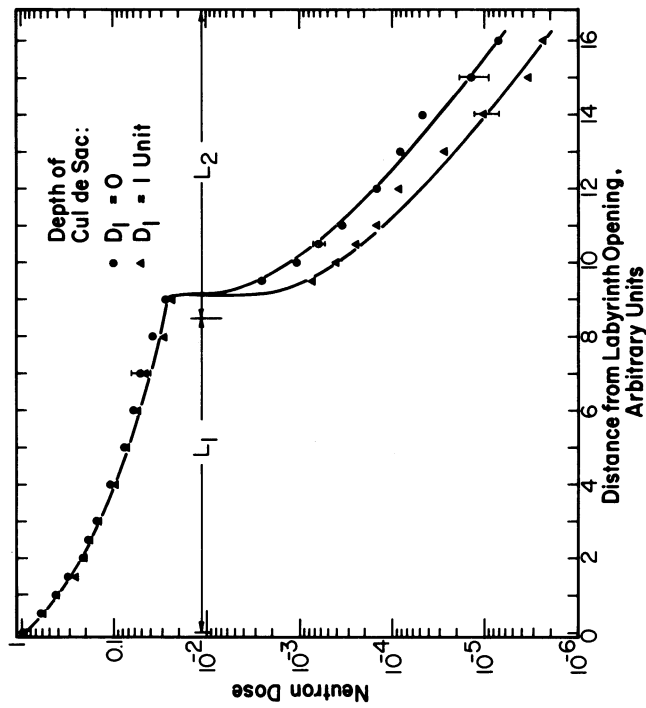


Fig. 7 Neutron dose for the same geometry as Fig. 6, but for $L_1 = 8.5\sqrt{A}$.

- viii) The first leg must be sufficiently long so that neutrons penetrating the bulk shielding will not be a problem in leg 3. In other words, a beam loss at point "B" of Fig. 1 should not cause more neutrons to reach the end of the second leg by penetrating the shielding than the same loss at point "A" would cause to reach that point by traveling down the first two legs of the labyrinth.
- ix) Each additional leg should be no longer than about $3\sqrt{A}$, it being more efficient to add more legs than to lengthen existing ones.

3.4 Multileg labyrinths: novel geometries

We also investigated the two novel cul-de-sac geometries shown in Fig. 9: a "tee" geometry in which the cul-de-sac is on the "wrong" wall, and a "box" geometry in which the cul-de-sac was enlarged to a small room at the intersection of the two legs. In both cases the labyrinth had a 2:1 aspect ratio, and the cul-de-sac had dimensions of one unit.

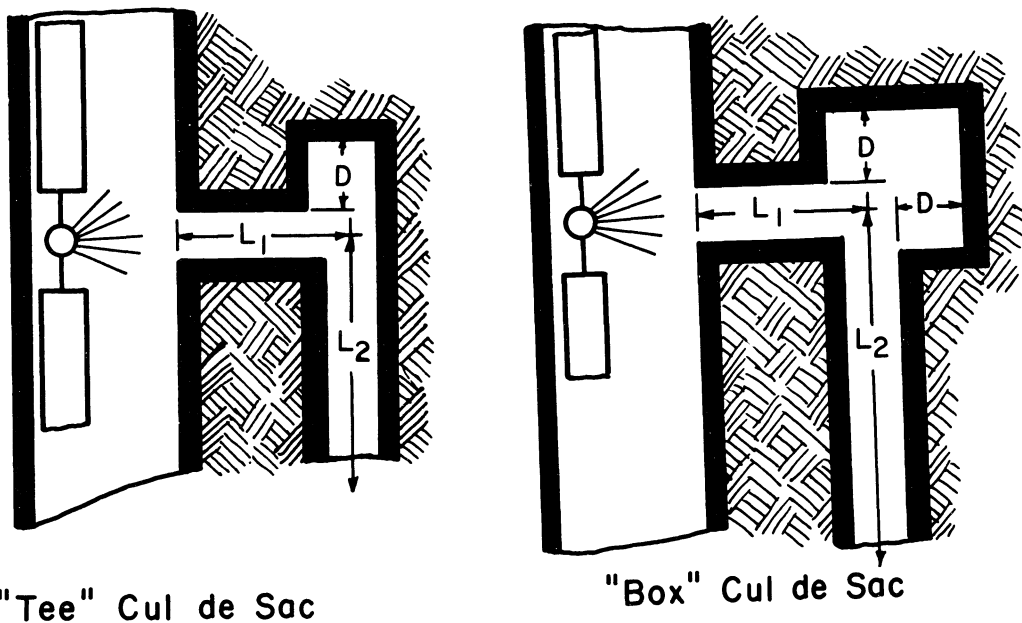


Fig. 9 Novel cul-de-sac geometries.

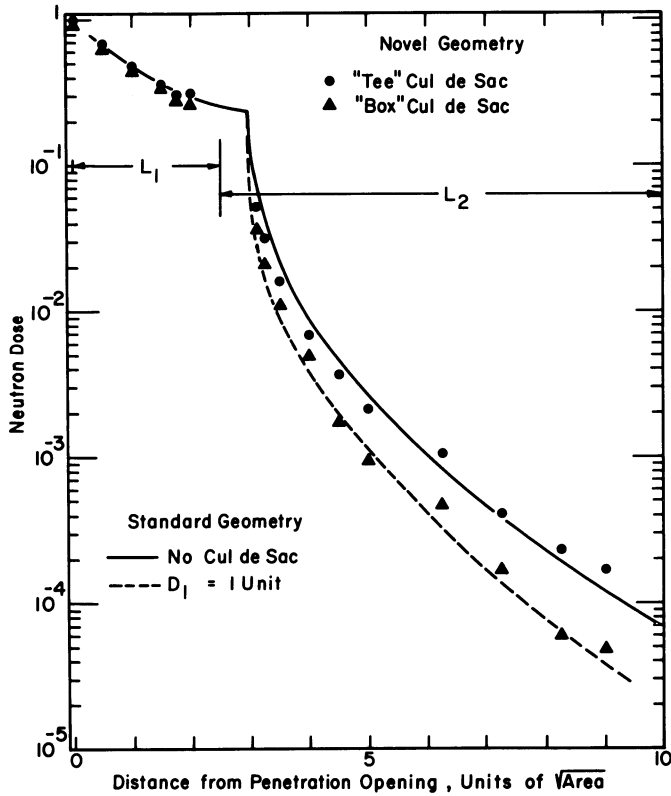


Fig. 10 Neutron dose in the first and second legs of labyrinths having the novel cul-de-sac geometries of Fig. 9.

The results are shown in Fig. 10. The "wrong" wall cul-de-sac produces no discernible effect on the attenuation. The "box" is not better than a conventional cul-de-sac one unit in depth.

3.5 Curved penetrations

When a penetration must accommodate large vehicles, it is not possible to use a multi-leg penetration, and continuously curved tunnels must be used. An example of such a situation is shown in Fig. 11, which shows a major vehicle entrance to the main accelerator enclosure. The major vehicle entrance consists of a semicircular tunnel with an 8 ft x 8 ft cross-section. The radius of curvature of the inner wall is 50 ft. Only particles produced in a backward direction from the proton beam can travel down the curved labyrinth for any significant distance. At the far end of the labyrinth there is a hoist shaft, stairway and elevator.

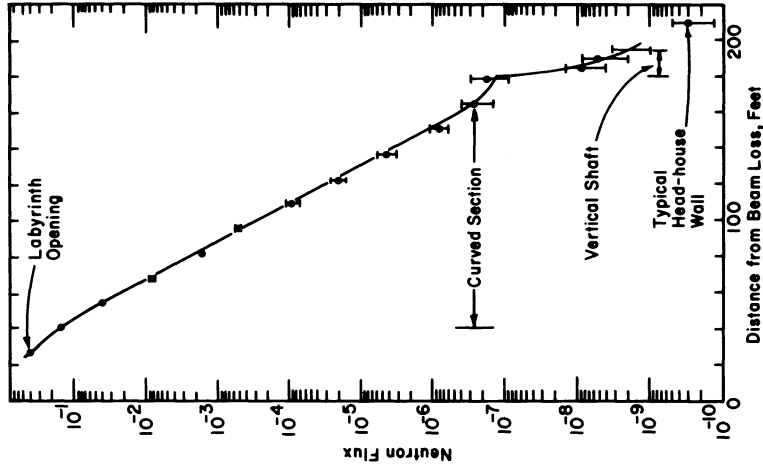


Fig. 12 Calculated neutron dose in the major vehicle access of Fig. 11.

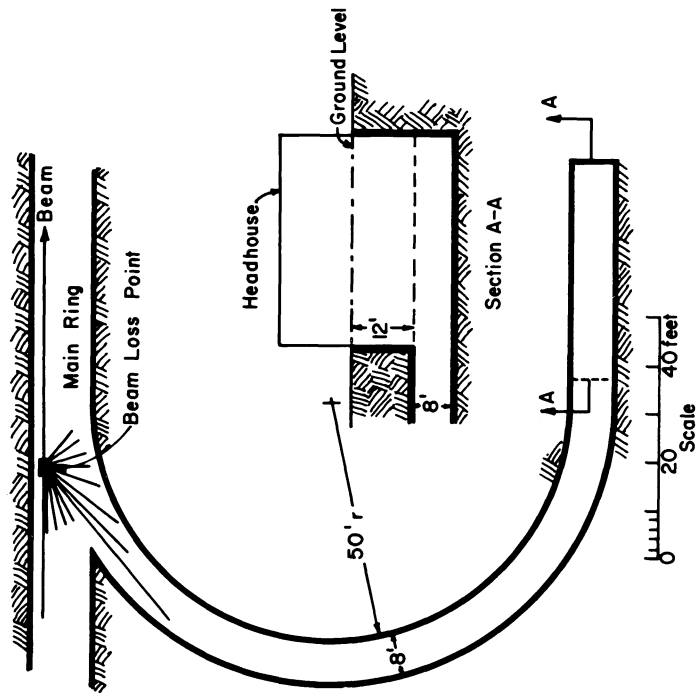


Fig. 11 Plans of a major vehicle access to the Main Accelerator enclosure.

For purposes of calculation, a beam loss was assumed to occur at a point on the beam line, just in front and upstream of the entrance to the labyrinth, as shown in Fig. 11. The calculated neutron fluxes at various distances down the centerline of the tunnel from the loss point are shown in Fig. 12. After a short transition region in which the loss point can be seen directly, the attenuation per foot of tunnel increases and remains constant throughout the curved region. The effect of the short straight section of tunnel before the shaft, and the sharp decrease in flux around the 90° bend formed by the shaft can also be seen. The overall attenuation of the labyrinth is defined as

$$A = \frac{\text{neutron dose into labyrinth opening}}{\text{neutron dose at floor of head house}} \geq 10^8$$

Thus, this design which was dictated by architectural considerations is quite adequate for the anticipated main ring beam losses^{1,16}).

A study of the dose attenuation of curved labyrinths of the same central radius, but two different cross-section areas and two different aspect ratios (Fig. 13) indicates that the angle through which the labyrinth turns has the greatest effect in determining its attenuation, and that (for realistic geometries) the height and width play a rather minor role.

We can write the dose as $D = c \cdot \exp(-\lambda(R,H,W) \cdot \theta)$, where R and θ are the central radius and angle around the labyrinth, and H and W are the height plus width of the labyrinth. Simple scaling says that λ depends only on the ratios $h=H/R$ and $w=W/R$: $\lambda = \lambda(h,w)$. Fig. 11 indicates that $\lambda(h,w)$ is a slowly varying function of h and w , increasing from 6.3 to 7.8 when the area of the labyrinth is doubled.

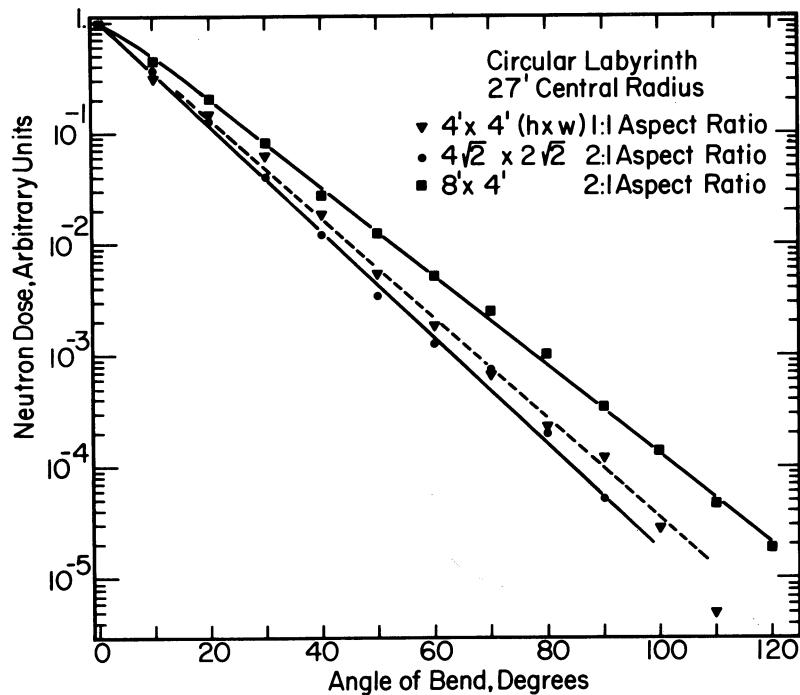


Fig. 13 Neutron dose at various locations around a circular labyrinth, for various cross-sections and aspect ratios.

* * * * *

REFERENCES

- 1) M. Awschalom, T. Borak, P. J. Gollon and D. Theriot, Radiation Physics Aspects of NAL Construction, NAL-FN-211 (1970).
- 2) M. Awschalom, Lateral Shielding for the 8-GeV and 200-GeV Synchrotrons, NAL-TM-241 (1970).
- 3) 1966 CERN-LRL-RHEL Shielding Experiment at the CERN Proton Synchrotron, UCRL-17941 (1968).
- 4) S. Charalambus, K. Goebel and D. Nachtigall, Angular Distribution of Secondary Particles and Dose Rates Produced by 19.2-GeV/c Protons on Thin Be, Al, Cu and U Targets, CERN Report DI/HP/97 (1967).
- 5) G. S. Levine, D. M. Squier, G. B. Stapelton and G. R. Stevenson, 300-GeV/RAD Note 70-22 (1970).

- 6) K. Goebel and J. Ranft, Radiation Measurements around a Beam Stopper....., CERN 70-16 (1970).
- 7) P. J. Gollon and M. Awschalom, Design of Penetrations in Hadron Shield, Proc. of 1971 Particle Accelerator Conf.
- 8) K. B. Shaw and G. R. Stevenson, RHEL/RPP/R6 (1969); and K. B. Shaw, private communication.
- 9) K. O'Brien, Transverse Shielding Calculations for..... A 1/2-TeV Proton Synchrotron, HASL-199 (1968).
- 10) R. G. Alsmiller, Shielding Calculations for a 200-MeV Proton Accelerator, ORNL-4336 (1968).
- 11) J. Ranft, Improved Monte Carlo Calculation....., CERN-MPS/Int. MU/EP 66-8 (1966).
- 12) A. Van Ginneken, Hadron Shielding Calculations: Effects of Voids, NAL-TM-287 (1971).
- 13) F. Gervaise, M.-M. d'Hombres, Variante du Programme ZEUS Appliquee à des Problemes de Tunnels: C.E.N. Fontenay-aux-Roses, Note CEA-N-933 (1968).
- 14) M.-M. d'Hombres, C. Devillers, F. Gervaise, B. de Sereville, PH. Tardy-Joubert, Propagation des Neutrons dans les Tunnels d'Acces à un Accelérateur de Haute Energie à Protons, GES.68.02-AIR.41-NC (1968).
- 15) R. E. Maerker, F. J. Muckenthaler, Calculation and Measurement of the Fast-Neutron Differential Dose Albedo for Concrete, Nucl Sci Eng 22, 465 (1965).
- 16) P. J. Gollon and R. A. Carrigan, Jr., NAL-TM-239 (1970).

DISCUSSION

Paper : On the design of penetrations through hadron shields

JENKINS: One of your curves, a two-legged duct, had superimposed a $1/R^2$ curve, which seems to be normalized at the far end of the duct ($\sqrt{A} = 20$). Would you comment on your reason for including this $1/R^2$ curve.

Also, it seems that, if the curve were slid up and normalized at the entrance point instead of the far end of the duct, the $1/R^2$ follows the calculation for a good distance, it would be nice if this were a universal phenomenon (which I doubt) for a single duct. Would you comment on this point.

GOLLON: The $1/R^2$ curve was normalized to the Monte-Carlo result at large distances from the source to illustrate the fact that at large distances most of the dose comes from neutrons which have not scattered from the walls, at smaller distances the deviation of the Monte-Carlo points from the $1/R^2$ curve shows that a larger portion of the dose is carried by neutrons which have scattered from the walls.

While the second comment does seem to be true (see Fig. 4), I can see no reason why it should be true in general.